

III Results:

3.1 Optimization of Biotinylation Reaction

3.1.1 Expression and Purification of BirA

3.1.1.1 Plasmid for BirA Expression

BirA was expressed as a GST-BirA fusion protein, the construction of Plasmid pGEX-BirA is shown in Fig. 9.

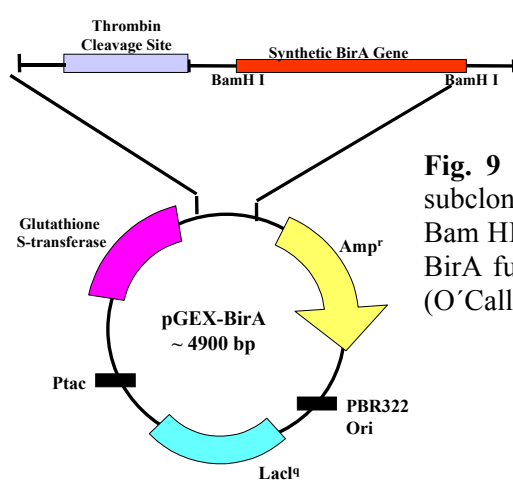


Fig. 9 Map of pGEX-BirA The synthetic BirA gene was subcloned into pGEX-2T vector at the restriction site of Bam HI, the resulting plasmid was shown to contain the GST-BirA fusion product with a define cleavage site for thrombin (O'Callaghan et al., 1999)

3.1.1.2 Expression and Purification of BirA

BirA was expressed as a GST-fusion protein, because addition of an N-terminal GST tag to the enzyme results in markedly enhanced expression compared with that of the untagged protein (Buoncristiani and Otsuka, 1988). N-terminal codon usage can influence RNA secondary structure and the probability of successful translation (Sorenson, 1988 and de Smit, 1994). The recombinant enzyme accounted for about 10% of total cellular protein, and up to 2 mg of purified enzyme can be obtained from 1 liter of bacterial culture. The use of the GST tag in conjunction with glutathione-Sepharose beads provided an efficient means for purification of the soluble recombinant protein. Solid-phase cleavage with

thrombin while the recombinant protein was bound to the beads liberated the free BirA moiety of the fusion protein at 4°C (Fig. 10). Thrombin was separated from BirA using gel filtration chromatography. (Fig. 11)

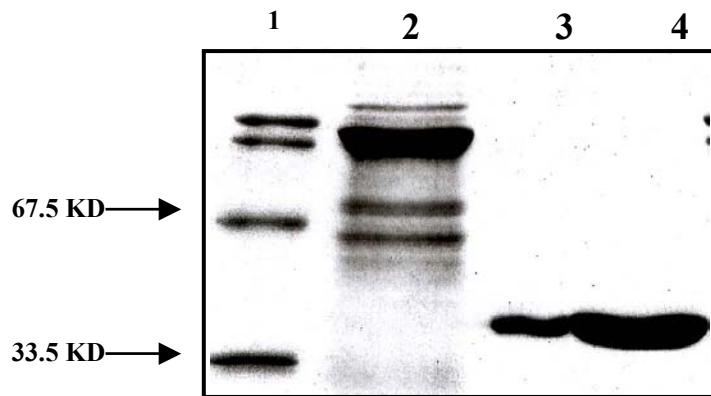


Fig. 10 SDS-PAGE of BirA Shows Different Fractions of Purification BirA was expressed in *E. coli*. BL21, the GST moiety was removed by cleavage with thrombin. (1) Molecular weight standard. (2) Eluted fusion protein (GST-BirA) without cleavage with thrombin. (3) BirA reference from Avidity (USA). (4) Expressed and purified BirA protein after cleavage with thrombin and removal of thrombin by gel filtration chromatography.

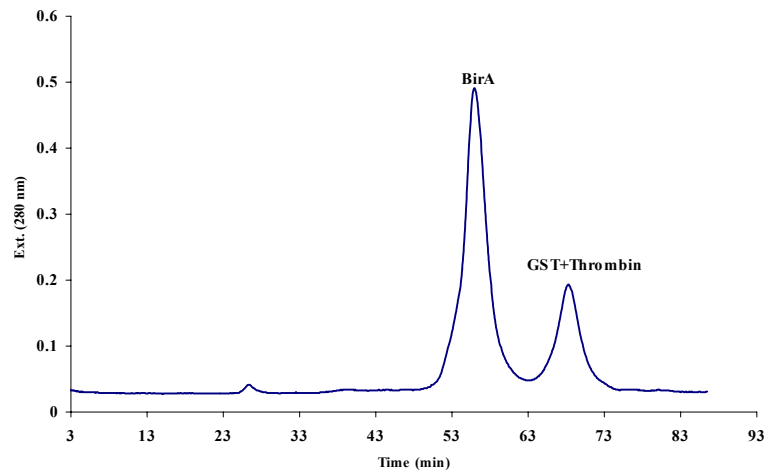


Fig. 11 Chromatography of BirA To remove the remaining contaminating proteins after cleavage, chromatography on a superdex 200 column was applied. The main protein peak of BirA showed a purity of about 95%

3.1.2 Expression and Purification of Biotinylated Maltose Binding Protein

A Maltose Binding Protein containing the biotinylation sequence at its C-terminus (MBP-Bio) was produced for the purpose to test the activity of expressed BirA and to optimize the reaction condition for biotinylation.

3.1.2.1 Construction of Plasmid for Biotinylated Maltose Binding Protein

The pMAL-C2x vector provides a method for expression and purification of a protein of interest fused in frame to the C-terminus of MBP. In the case of MBP-Bio, the consensus sequence of 13 amino acid was inserted downstream from the *malE* gene of *E. coli*, which encodes maltose-binding protein (MBP) (Fig. 13), resulting in the expression of an MBP-Bio fusion protein (Guan et al., 1987 and Kellerman, 1982).

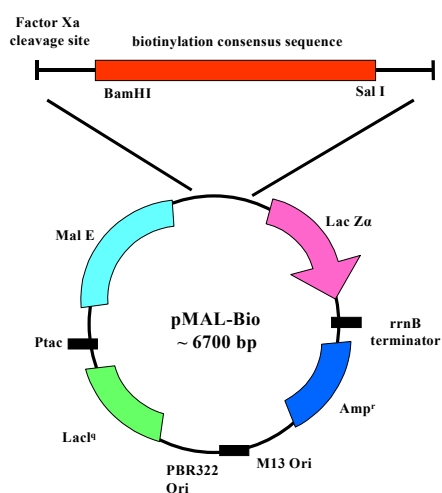


Fig. 13 Map of pMAL-Bio The vector pMAL-c2x was digested with BamHI and SalI, the biotinylation consensus sequence (Bio) was cloned into the digested vector.

3.1.2.2 Expression, Biotinylation and Purification of MBP-Bio

The pMAL-C2x uses the strong 'tac' promoter and the malE translation initiation signal to give high-level expression of the cloned sequences (Amann, 1985), and allows one-step purification of the fusion protein using MBP's affinity for maltose.

After purification of MBP-Bio via an amylose resin column, the biotinylation reaction was performed by adding BirA, ATP, pyrophosphate and biotin, followed by incubation at room temperature overnight with gentle agitation.

The free biotin was removed through gel filtration and the purified bionylated MBP-Bio was obtained by purification via monomeric avidin column. The non-biotin-tagged protein was contained in the flow-through and wash fractions, biotinylated protein was bound to the resin. The biotin-tagged MBP was eluted with a buffer containing 5 mM biotin (Fig. 14).

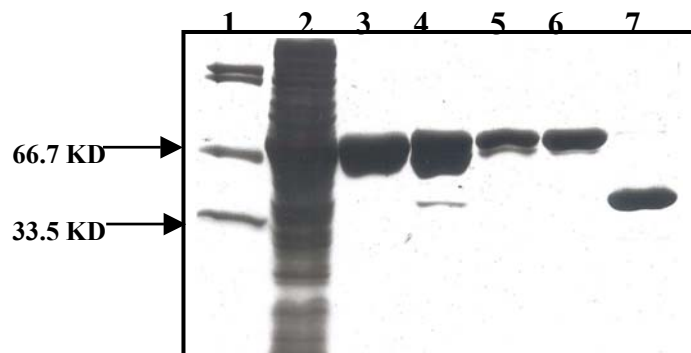


Fig. 14 Expression and Purification of MBP-Bio Biotinylated MBP-Bio was expressed in *E. coli* BL21. SDS-PAGE showing different products in the sequence of expression and purification of a C-terminally biotin-tagged MBP: Lane (1) Molecular weight standard. (2) *E. coli* cells lysed after induction with IPTG. Lane (3) Elution of MBP-Bio from Amylose resin. (4) Flow through of in vitro biotinylated MBP-Bio fusion protein applied to a monomeric avidin column. Lane (5) Wash fraction of monomeric avidin column, mainly containing non-biotinylated protein. Lane (6) Elution of purified biotinylated MBP-Bio from the monomeric avidin column with 5 mM biotin in equilibration buffer. Lane (7) BirA as reference.

3.1.3 Optimization of Biotinylation Reaction Conditions

Enzymatic biotinylation is a post-translational modification of extraordinary specificity. Biotin attachment is a two-step reaction that results in the formation of an amide linkage between the carboxyl group of biotin and the ϵ -amino group of the modified lysine (McAllister and Coon, 1966) (Fig. 6).

To maximize the amount of biotin-tagged protein, the conditions of the biotinylation reaction had to be optimized.

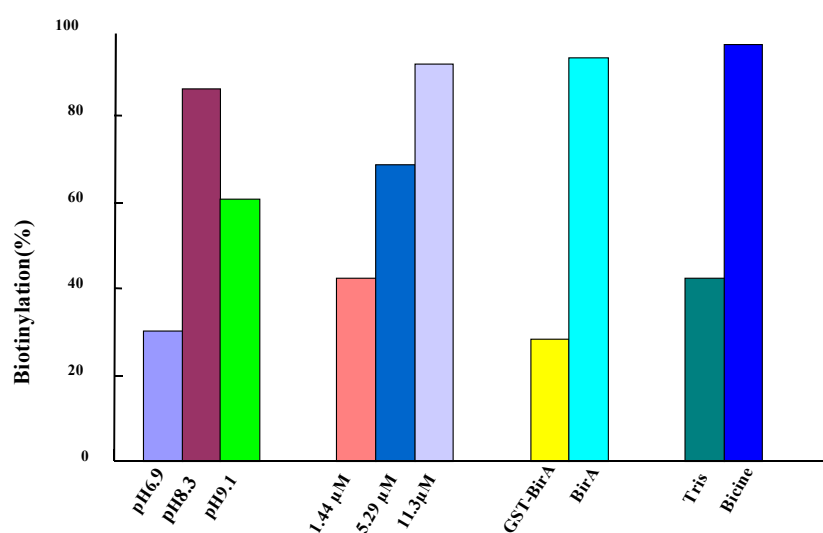


Fig. 15 Optimization of Biotinylation Reaction The biotinylation reaction was performed at room temperature over night with MBP-Bio at different pH (6.9; 8.3; 9.1), different reaction buffers (Bicine; Tris-base, pH 8.3), different concentration of MBP-Bio (1.44 μ M; 5.29 μ M; 11,3 μ M) and the activity of BirA was compared to GST-BirA.

The pH value, Concentration of the peptide, and buffer (bicine/Tris) used were tested, the activity of BirA was compared to GST-BirA. The yield of biotinylation is as following: 42.3% for Tris Buffer (pH 8.3), 94.6% for Bicine buffer (pH 8.3); Biotinylation varied with pH: 86.4% (pH 8.3), 30.2% (pH 6.9) and 60.7% (pH 9.1). Also the concentration of MBP-Bio substrate is a critical factor of the biotinylation reaction, 90.8% biotinylation can be obtained with a MBP-Bio concentration of 11.3 μ M, compare to 42.3% for 1.44 μ M

and 68.6% for 5.29 μ M. In addition, the biotinylation is improved after cleavage of the MBP-BirA fusion by thrombin (91.6% biotinylation for purified BirA, 28.4% for GST-BirA) (Fig. 15).

3.2 Biotinylation of Recombinant Rhodopsin

3.2.1 Recombinant Rhodopsin with Biotinylation Sequences

Three rhodopsin mutants with a 13-aa acceptor peptide, which can be recognized by BirA were expressed in COS cells and purified.

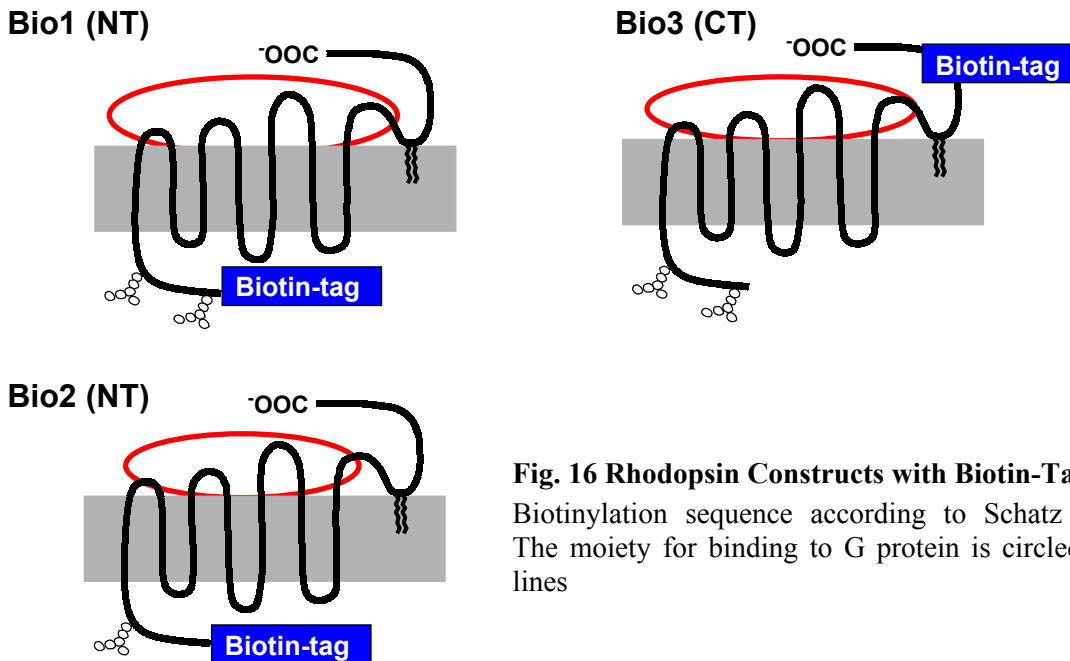


Fig. 16 Rhodopsin Constructs with Biotin-Tags
Biotinylation sequence according to Schatz (1993).
The moiety for binding to G protein is circled in red lines

Amino acid sequences:

WT:		MNGTEGP-----S	TTVSKTETSQQVAPA
Rho-Bio1:	MGLNDIFEAQKIEWHE	MNGTEGP-----S	TTVSKTETSQQVAPA
Rho-Bio2:	MGLADIFEAQKIEWHE	-----GTEGP-----S	TTVSKTETSQQVAPA
Rho-Bio3:		MNGTEGP-----SGLADIFEAQKIEWHE	TTVSKTETSQQVAPA

*Rhodopsin sequence is indicated in purple and biotin-tag in blue

The 13-aa acceptor peptide was fused to the N-terminus of rhodopsin, the difference between the mutants Rho-Bio1 and Rho-Bio2 is a deletion of a glycosylation site close to the N-terminus in Rho-Bio2. In the Rho-Bio3 control mutant, the same biotinylation sequence was introduced close to the C-terminus. The biotinylation sequence was not fused directly to the C-terminus because an unmodified free C-terminus is necessary for the purification of rhodopsin with the 1D4 antibody-column (Fig. 16).

3.2.2 Construction of Plasmid pMT-Rho

The expression vector pMT4 containing the synthetic rhodopsin gene was used to construct the gene encoding rhodopsin with a consensus sequence for the biotin tag at the N-terminus or close to the C-terminus (Fig. 17).

3.2.3 Expression, Purification and Biotinylation of Rho-Bio

COS-1 cells were transfected with the plasmid of recombinant opsin, 72 hours past transfection, these cells were harvested and the pigment was reconstituted by incubation with 11-*cis*-retinal. The rhodopsins were purified by immunoaffinity adsorption based on a procedure of Oprian et al (1987). Elution of the pigments from the 1D4-Sepharose was carried out in elution buffer supplemented with 100 μ M peptide corresponding to the carboxyl-terminal 18 amino acids of rhodopsin.

The fraction of elution was concentrated to the final concentration of ~ 10 μ M, mixed with BirA, ATP, pyrophosphate and biotin, incubated at room temperature overnight with gentle agitation.

After biotinylation, the free biotin was discarded through gel filtration and the purified bionylated rhodopsin was obtained by purification via monomeric avidin column. The non-biotin-tagged rhodopsin flew through the column, while the biotin-tagged rhodopsin bound to the resin can be eluted with biotin solution with the concentration of 5 mM (Fig. 18).

Another protocol for biotinylation is to perform the reaction during the purification procedure. After expression rhodopsin was bound to 1D4-Sepharose, the gel was washed two times with PBS and Bicine, and incubated with BirA, ATP, pyrophosphate and biotin,

at room temperature overnight with gentle agitation. Then, the gel was washed two times with PBS, one time with BTP buffer. The biotinylated rhodopsin was then eluted with 100 μ M peptide in BTP buffer.

The major advantage of this protocol is that, free biotin and biotinylation buffer can be removed easily before elution, but the yield of biotinylation is smaller (~60%) compared to biotinylation of unbound rhodopsin (90%).

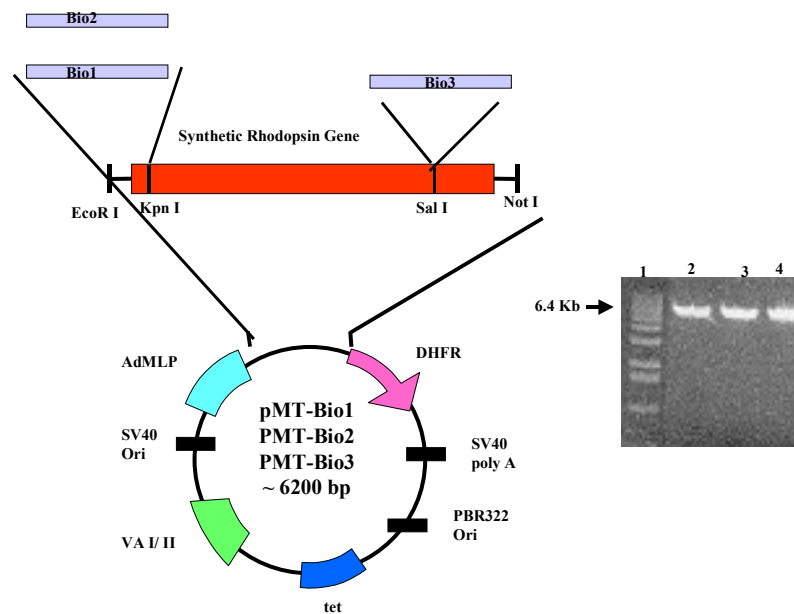


Fig. 17 A Schematic Diagram Showing the Construction of Plasmid pMT-Bio1, pMT-Bio2 and pMT-Bio3

(A) The EcoRI-KpnI restriction fragment was replaced by synthetic oligonucleotide duplexes to obtain plasmids PMT-Bio1 and PMT-Bio2. For construction of plasmid PMT-Bio3, PMT4 was digested with SalI and a synthetic oligonucleotide duplex encoding the biotinylation sequence was inserted.

(B) Agarose gel of EcoRI digested plasmids: Lane 1: standard, Lane 2: PMT-Bio1, Lane 3: PMT-Bio2, Lane 4: PMT-Bio3.

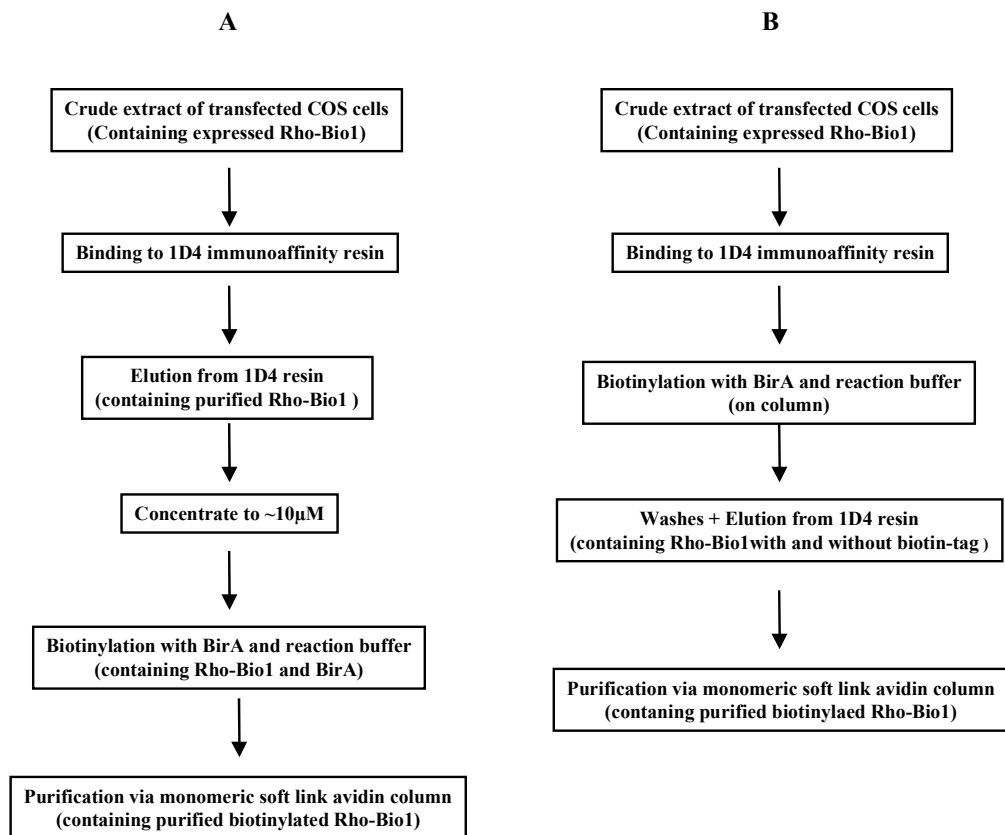


Fig. 18a Two Different Protocols for Biotinylation of Rhodopsin

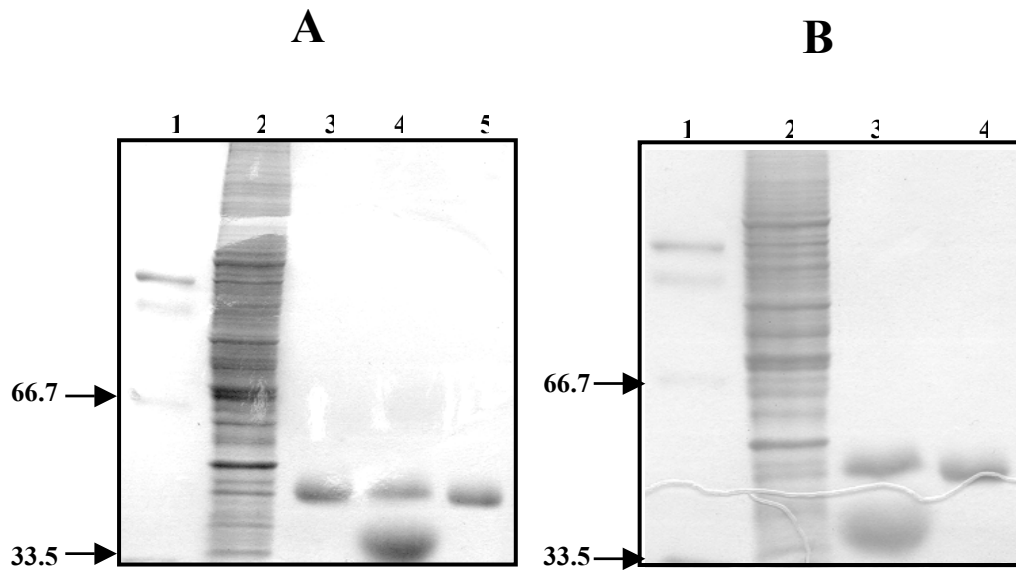


Fig. 18b SDS-PAGE Monitoring Purification Steps in the Course of Biotinylation of Rho-Bio1 SDS-PAGE was used to monitor purification steps in the course of biotinylation of Rho-Bio1: A: Biotinylation of solubilized rhodopsin: (1) molecular weight standard, (2) crude extract of transfected COS cells. (3) Soluble Rho-Bio1 after purification with 1D4 immunoaffinity resin, (4) Biotinylation mixture containing purified Rho-Bio1 and BirA. (5) Biotinylated Rho-Bio1 purified via monomeric soft link avidin column. B: Biotinylation of rhodopsin bound to 1D4 resin: (1) molecular weight standard, (2) crude extract of transfected COS cells. (3) Biotinylation performed with Rho-Bio1 bound to resin. (4) Eluted Rho-Bio1 from 1D4 resin in elution buffer supplemented with 100 μ M peptide corresponding to the carboxyl-terminal 18 amino acids of rhodopsin

3.3 Quantification of Biotinylation

3.3.1 Evaluation by Western Blotting

Western blotting was used to detect biotinylation of wild type rhodopsin and mutants Rho-Bio1, Rho-Bio2 and Rho-Bio3. The rho 1D4 monoclonal antibodies, which is specific for C-terminal sequence of rhodopsin, and anti-biotin antibody which is specific for biotin, were applied (Fig. 19). The western blotting of the biotinylation reaction mixture containing rhodopsin mutants and BirA shows that biotin is exclusively incorporated into Rho-Bio1, Rho-Bio2 and Rho-Bio3 but not into wild type rhodopsin.

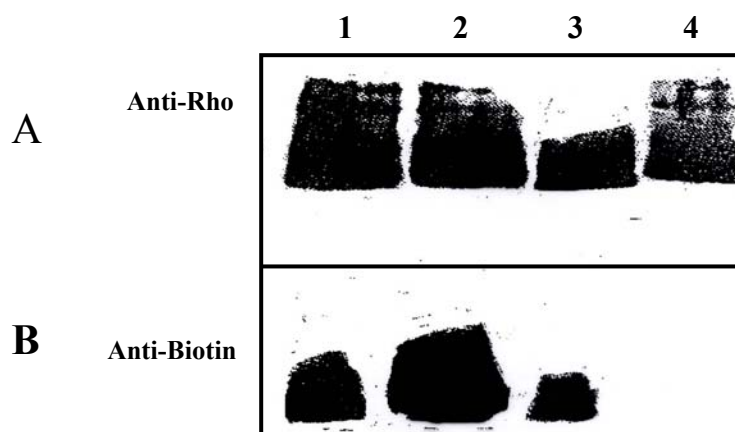


Fig. 19 Western Blotting of Biotinylation Biotinylation was performed with solubilized Rho-Bio mutants, the biotinylation mixture and wild type rhodopsin were solubilized in SDS-sample buffer, loaded and separated by discontinuous SDS-PAGE under reducing conditions respectively, thereafter, proteins were electrophoretically transferred onto NC membranes (Protran BA85, 0.45 μ m) and incubated with antibodies. Antibody of 1D4 (shown in A) was directed against the nine C-terminal amino acids of rhodopsin and anti-biotin (shown in B) respectively. Lane 1: Rho-Bio1; Lane 2: Rho-Bio2; Lane 3: Rho-Bio3 and Lane 4: wild type rhodopsin

3.3.2 Quantitation of Biotinylation

Streptavidin sepharose was used to quantitate the amount of biotinylated rhodopsin. After the biotinylation reaction the mixture was applied to streptavidin agarose. Due to the strong affinity of streptavidin to biotin ($K_d=10^{-15}$), only biotinylated rhodopsin binds to it, non-biotinylated rhodopsin remains in the flow-through. By measuring the absorption of rhodopsin in the flow-through and wash fractions, the amount of rhodopsin which did not bind can easily be determined and the difference to the sample applied can be calculated. The values are shown in Fig. (20): Only about 1 % of wild type bound to the column suggesting that wild type rhodopsin does not have a biotin modification. In the case of the Rho-Bio mutants the biotinylation reaction was successful, yielding 94% of biotinylated Rho-Bio1, 97% for Rho-Bio2 and 61% for Rho-Bio3.

In another experiment, the biotinylated rhodopsin was applied to streptavidin resin and washed, the resin was boiled in SDS-sample buffer to remove the biotinylated rhodopsin and subjected to SDS-PAGE (Fig. 21). It shows that only in the lanes with the Rho-Bio mutants rhodopsin can be detected but no signal in the lane with wild type rhodopsin.

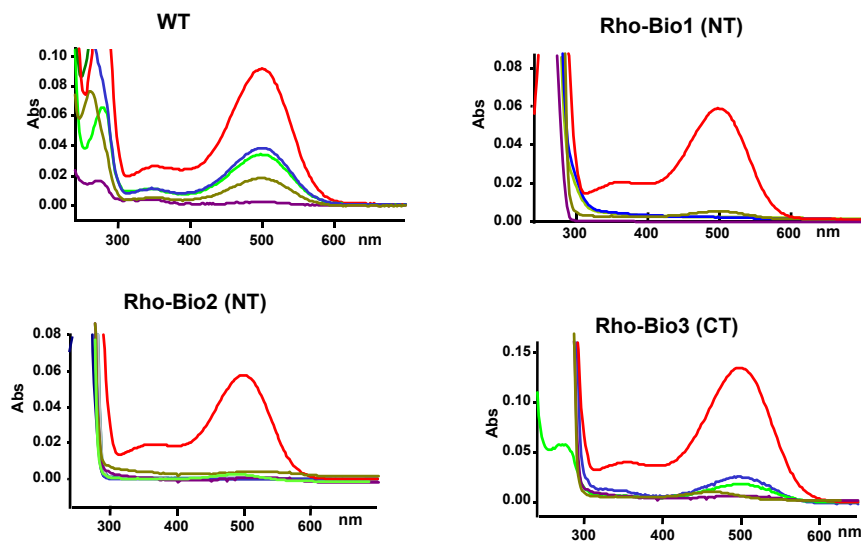


Fig. 20 Analysis of Biotinylation by UV/Vis Spectroscopy

After biotinylation of solubilized Rho-Bio mutants, the biotinylation reaction mixture or wild type rhodopsin were mixed with 50 μ l streptavidin resin in PBS buffer(0.1% DM) and allowed to bind to streptavidin resin. The flow-through and wash fractions were collected and UV/vis spectra measured. The sample applied to the resin (200 μ l) is shown in red; The flow-through (200 μ l) is shown in yellow; Wash 1 (200 μ l) is shown in blue; Wash 2 (200 μ l) shown in green; Wash 3(200 μ l) shown in pink.

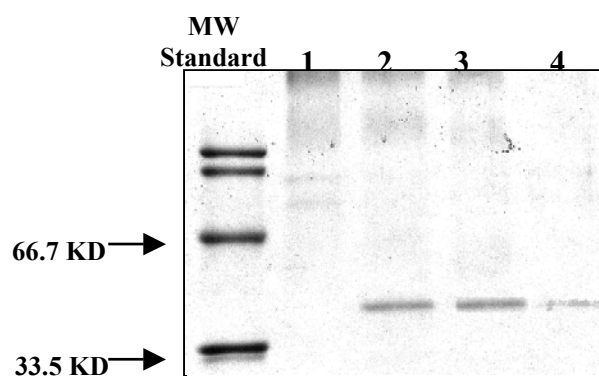


Fig. 21 SDS-PAGE of Rhodopsin Bound To Streptavidin resin The streptavidin resin (See Fig. 20) was washed and boiled in SDS-sample buffer. The sample containing proteins removed from the resin was applied to SDS-PAGE. Lane 1: wild type rhodopsin, Lane 2: Rho-Bio1, Lane 3: Rho-Bio2, Lane 4: Rho-Bio3.

3.4 Characterization of Rhodopsin-Bio Mutants

After biotinylation, Rho-Bio mutants were purified using monomeric avidin chromatography and characterized.

3.4.1 UV/Visible Absorption Spectroscopy

All Rho-Bio mutants showed a λ_{\max} value of 498 nm in the dark. After illumination, photolysis of rhodopsin resulted in a complete photoconversion to MII ($\lambda_{\max} = 380\text{nm}$). (Fig. 22)

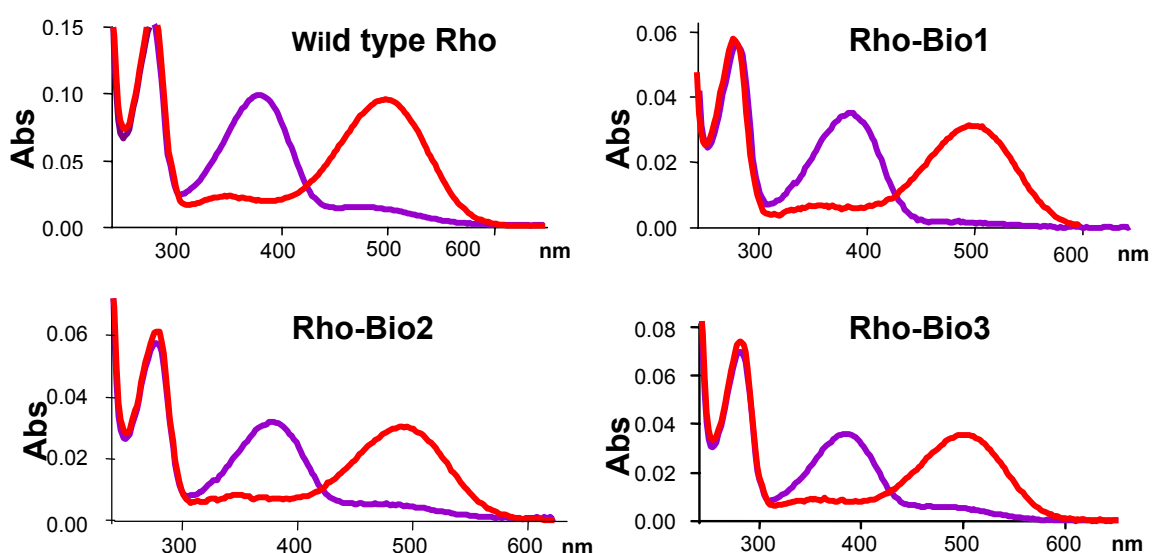


Fig. 22 UV/vis Spectra of Biotinylated Rhodopsin Mutants Spectra of biotinylated rhodopsins were measured in the dark (shown in red), and after illumination (shown in purple) for 15 s with $\lambda \geq 480$ nm. The buffer used was BTP buffer with 0.03% DM.

3.4.2 The Activation of Transducin Determined with Fluorescence Assay

Next it was tested whether the biotinylation affects the capability of rhodopsin to catalyze nucleotide exchange in transducin. Catalytic amounts of light-activated rhodopsin catalyze the nucleotide exchange in the G-protein. The cuvette contains rhodopsin and G protein

and the reaction is started by the addition of GTP γ S, a non hydrolyzable analog of GTP (Fig. 23).

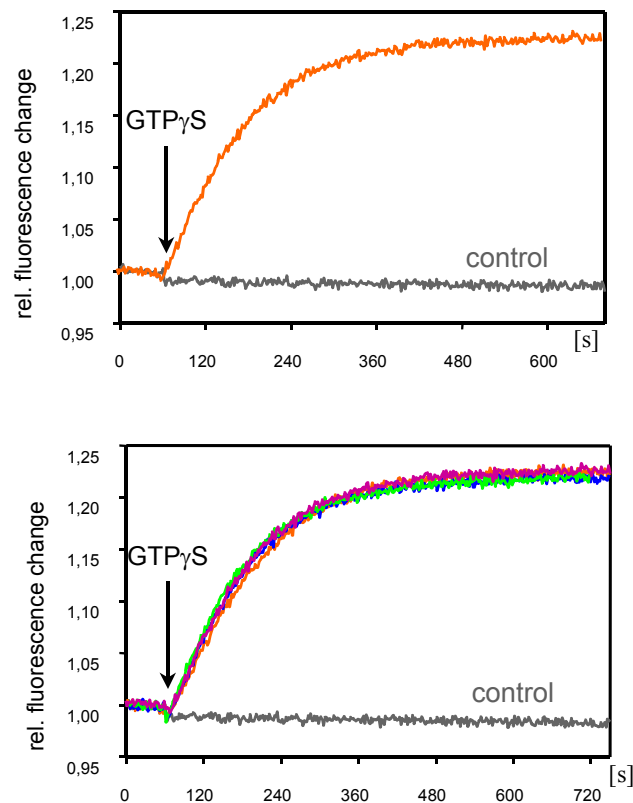


Fig. 23 Fluorescence Assay Wild type rhodopsin and purified biotinylated Rho-Bio mutants (2 nM) were reconstituted with 250 nM Gt, 20 mM BTP, pH 7.5, 130 mM NaCl, 1 mM MgCl₂. The samples were mixed in the dark, and Gt activation was initiated by injection of GTP γ S to a final concentration of 5 μ M. Traces of Gt activation are a percent change of fluorescence emission at 345 nm recorded with excitation of the sample at 300 nm. Wild type rhodopsin is shown in yellow, Rho-Bio1 in blue, Rho-Bio2 in green and Rho-Bio3 in pink.

When GTP uptake by the G-protein occurs, the G protein dissociates into its subunits which causes an increase in Trp²⁰⁷ fluorescence of α (Faurobert et al., 1993). This is not seen in the control where rhodopsin is missing. The initial rate of the fluorescence change after GTP addition can be used to compare the activity of rhodopsin mutants towards the G protein.

It can be seen that the trace for wild type rhodopsin and the purified Rho-Bio mutants are almost identical. As expected, the biotinylation does not affect the activity of rhodopsin at the N-terminus. Interestingly also biotinylation in Rho-Bio3, at the C-terminus does not affect Rho-Bio3 activity.

3.4.3 Interaction between Rhodopsin and Transducin

Photoactivation of rhodopsin causes binding of R* to transducin, subsequent addition of GTP γ S leads to dissociation of the R*·G complex and dissociation of G protein into subunits. Binding of Gt to rhodopsin of Rho-Bio which bound to 1D4 resin or streptavidin resin separately, is followed by SDS-PAGE. Protocols and results are shown in Fig. (24).

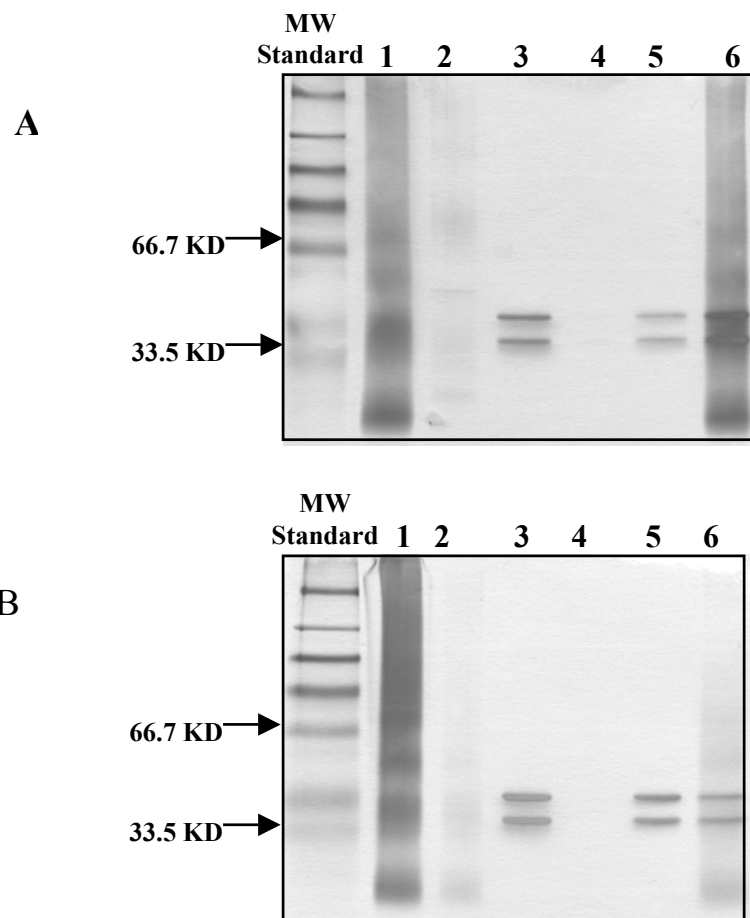


Fig. 24 Binding of Transducin To Rhodopsin Immobilized via 1D4 or Biotin Tag (SDS-PAGE followed by Silver Staining) (A) Biotinylated rhodopsin: Biotinylated Rho-Bio1 ($1\mu\text{M}$) was bound to streptavidin resin (lane 1, sample applied). The resin was washed with BTP buffer (lane 2, wash fraction). Then the resin was incubated with $3.5\mu\text{M}$ transducin (lane 3, unbound fraction of Gt), and the resin washed with BTP buffer (lane 4, wash fraction). One half of the washed resin was incubated with $20\mu\text{M}$ $\text{GTP}\gamma\text{S}$ to elute Gt (lane 5), the other half was boiled in SDS loading buffer to remove R^* -bound Gt (lane 6).

(B) Wild type rhodopsin: Wild type rhodopsin ($1\mu\text{M}$) was incubated with 1D4 resin (lane 1, sample applied) over night and then washed with BTP buffer (lane 2, wash fraction). The resin was incubated with $3.5\mu\text{M}$ transducin (lane 3, unbound fraction of Gt), and the resin washed with BTP buffer (lane 4, wash fraction). One half of the washed resin was incubated with $20\mu\text{M}$ $\text{GTP}\gamma\text{S}$ to elute Gt (lane 5), the other half was incubated with $100\mu\text{M}$ 1D4 peptide to elute R^* -bound Gt (lane 6).

3.5 Interaction between Gt and Rho-Bio1 Monitored by the IAsys system

The experiment with the IAsys system includes immobilization of rhodopsin onto the sensor chip, reconstitution of the immobilized rhodopsin into a lipid bilayer and measurement of Gt activation. The procedure is shown in Fig. 25.

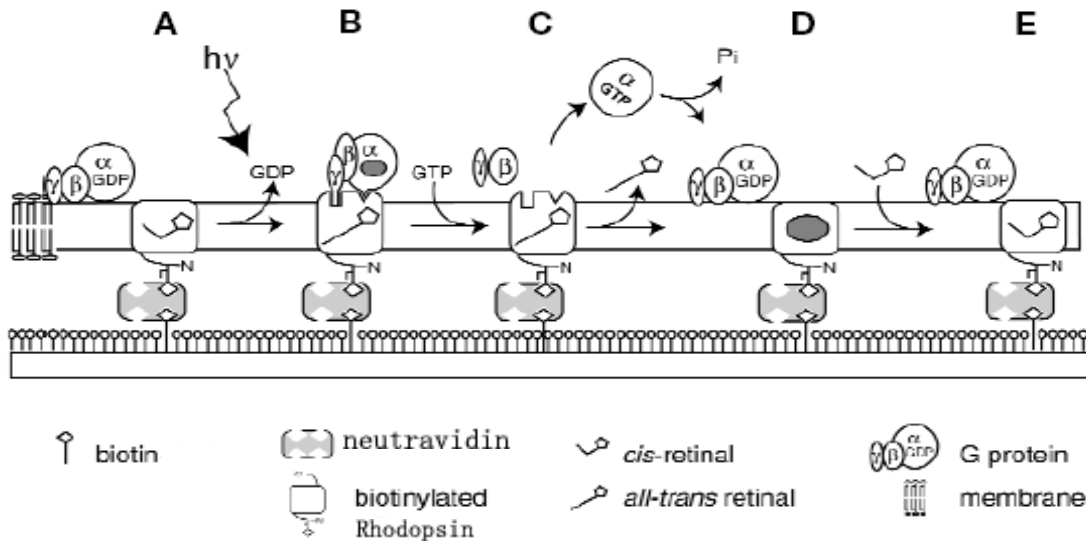


Fig. 25 The Principle of the Assay for Rhodopsin and Gt Activation Using IAsys System

(Adapted from Bieri et al., 1999)

- Immobilization of the receptor. NeutrAvidin binds to the biotin-derivatized sensor chip and docks biotinylated rhodopsin to the surface. Site-specific biotinylation of the latter results in uniform orientation of the bound rhodopsin. The G protein binds to the supported lipid bilayer, which is formed after receptor immobilization.
- Photoisomerization of 11-*cis*- to all-*trans*-retinal triggers the active conformation of rhodopsin. G protein bound to light-activated rhodopsin liberates its GDP and
- desorbs from the membrane upon GTP binding, leading to a decrease in mass charge on the sensor chip that can be followed by the IAsys system.
- Active rhodopsin decays spontaneously to all-*trans*-retinal and opsin, and the G protein binds after nucleotide hydrolysis again to the surface.
- 11-*cis*-retinal binds to opsin, and regenerates photoactivatable rhodopsin.

3.5.1 Immobilization of Biotinylated Rhodopsin

3.5.1.1 Monolayer of NeutrAvidin Linker

The IAsys cuvettes are modified with biotin, which allow rapid, efficient, and tight capture of a monolayer of avidin. The unoccupied biotin-binding sites on the avidin may then be used to capture biotinylated protein.

As a deglycosylated form of avidin, NeutrAvidin™ Biotin-Binding Protein was applied to achieve better assay results due to its lower nonspecific binding property (Wojciechowski, et al., 1999). The cuvette was rinsed for 10 minutes, and mounted to the instrument of the IAsys system, then all subsequent immobilization steps followed.

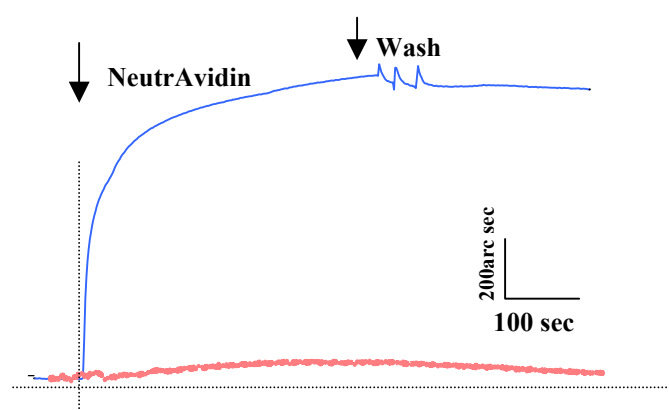


Fig. 26 Sensorgram of NeutrAvidin Binding Monitored with the IAsys System NeutrAvidin was added to the biotin-coated cuvette to a final concentration of 200 nM (indicated by arrow). Then the cuvette was washed with buffer R (containing 0.01% DM, indicated by second arrow). Traces of two different experiments are shown: NeutrAvidin in blue and biotin-presaturated NeutrAvidin in red.

NeutrAvidin was added in buffer R to a final concentration of 200 nM, and allowed binding to occur for 10 minutes, which lead to a fast increase in the resonance angle, induced by its binding to the biotin-coated sensor surface (Fig. 26). NeutrAvidin binding resulted in an angle shifts of 1241 ± 96 arc sec (N= 10), NeutrAvidin which was presaturated with biotin, induced no binding signal. According to the manufacturer, the

sensitivity of the biotin cuvette is $600 \text{ arc sec per ng/mm}^2$, which can be used to calculate the density of protein immobilized.

3.5.1.2 Immobilization of Biotinylated Rhodopsin

In a primary experiment, biotinylated MPB-Bio was applied to the NeutrAvidin monolayer by addition of MBP-Bio to the cuvette containing immobilized NeutrAvidin. The biotin-tagged MBP induced a significant increase in angle shift, compared to the non-bio-tagged MBP, which showed only a minor binding signal, indicating the specificity of surface-immobilized NeutrAvidin.

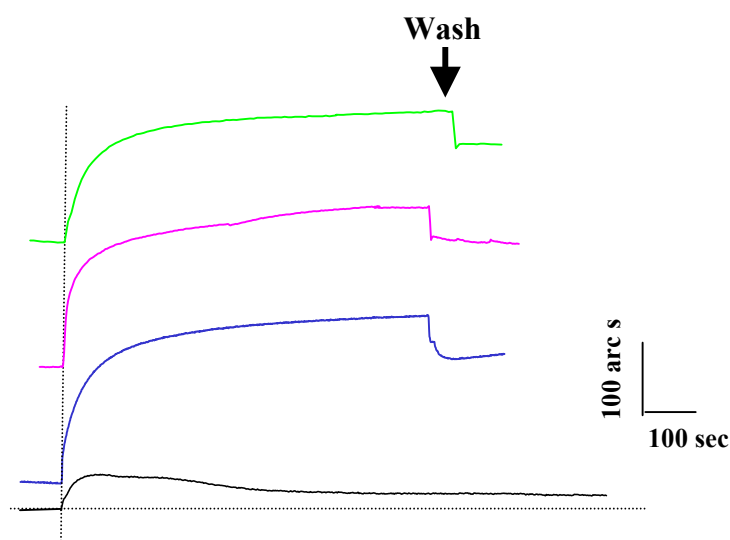


Fig. 27 Sensorgram of Immobilization of Biotinylated Rhodopsin Addition of $1 \mu\text{M}$ Rho-Bio mutants to the avidin-coated sensor surface, leads to an increase of the resonance angle. Biotinylated Rho-Bio1 is shown in green, Rho-Bio2 is shown in pink and Rho-Bio3 is shown in blue, non-biotin wild type rhodopsin is shown in black

Biotinylated Rho-Bio mutants were injected to the cuvette with immobilized NeutrAvidin to a final concentration of $1 \mu\text{M}$ (Fig. 27). This led to a fast increase, saturating after 600 sec. Washing with buffer R 3 times removed unspecifically adsorbed rhodopsin and yielded a resonance angle shift due to rhodopsin binding of $345 \pm 52 \text{ arc sec}$ ($N = 7$). The amplitudes of the binding traces obtained with Rho-Bio1, Rho-Bio2 and Rho-Bio3 are

similar and significantly higher than wild type rhodopsin compared to non-biotinylated rhodopsin.

3.5.2 Formation of Supported Lipid Bilayers

After immobilization of rhodopsin, the cuvette was washed with 200 μ l of buffer OG50 containing 1 mg/ml egg phosphatidylcholine (EPC), resulting in a small increase of the resonance angle. Meanwhile, the cuvette was slowly and under constant stirring diluted with G buffer (without detergent) until the OG50/EPC solution was diluted 1:3 (Fig. 28).

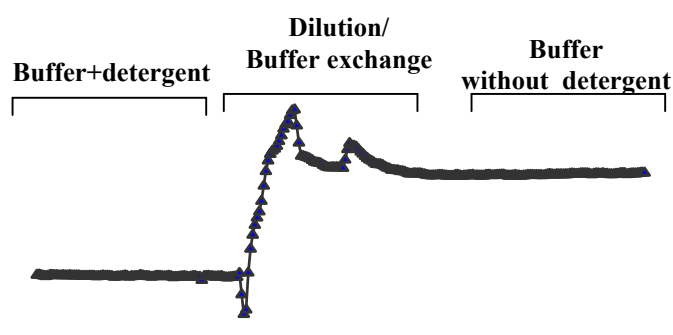


Fig. 28 Sensorgram of Supported Lipid Bilayer Formation A supported lipid bilayer (SLB) was formed by micellar dilution. This lead first to a decrease, then to a fast increase of response, which slowly decreased again, reaching a stable value after some minutes. The fast increase of the resonance angle has been shown to occur approximately when the detergent is diluted below the critical micellar concentration (cmc) and the membrane starts to form (Lang et al., 1994). Further washing (exchange of solution in the cuvette with buffer (without detergent)), even with large volumes over long time did not alter the response, indicating that the supported lipid bilayer is stable.

3.5.3 Detection of Immobilized Rhodopsin by Antibody

After formation of the supported lipid bilayer, 1D4 antibody was injected to the cuvette to detect rhodopsin in SLB. When antibody was added to the final concentration of 0.1% (v/v), angle shifts of 28.9 arc sec for Rho-Bio2 and 24.6 arc sec for Rho-Bio1 were observed, which are significantly higher than that of Rho-Bio3 (Fig. 29). Further addition of antibody and/or exchange of solution in the cuvette with buffer (washes) did not change the response values, indicating that antibody binding was saturating and stable.

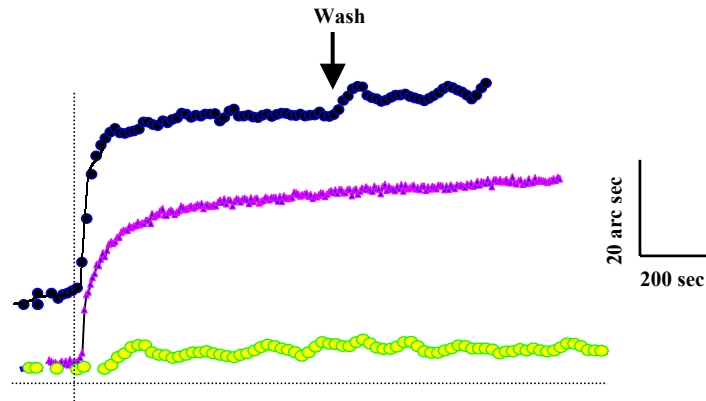
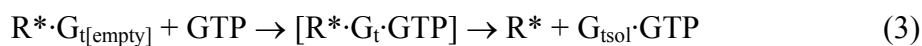


Fig. 29 Sensorgram of Binding of 1D4 Antibody to Immobilized Rhodopsin Incorporated into A Supported Lipid Bilayer Binding traces are shown for: Rho-Bio1 (blue), Rho-Bio2 (pink), Rho-Bio3 (yellow). The arrow indicates when buffer exchange (wash) steps were performed.

3.5.4 Rhodopsin-G protein Interaction

3.5.4.1 Transducin Activation Reaction Scheme

The interaction between active rhodopsin (R^*) and transducin (G_t) is based on the following reaction sequence (Ernst et al., 2000):



Step 1 describes the equilibrium of the inactive GDP-bound G_t , which is distributed between a soluble ($G_{tsol} \cdot GDP$) and a membrane-bound fraction ($G_{tmb} \cdot GDP$) (Liebman et al., 1987). In the micromolar range, binding of G_t to the membrane occurs within a few seconds with an apparent K_D of 10^{-5} - 10^{-6} M (Schleicher et al., 1987). Similar rates are measured in detergent solution where the rate of $R^* \cdot G_t$ formation may depend on the transition of G protein from detergent micelles to the solubilized rhodopsins (Ernst et al., 2000).

Step 2 describes the formation of the nucleotide-free complex between R^* and Gt ($R^* \cdot G_{t[\text{empty}]}$). liberation of GDP by $R^* \cdot G$, can be shown directly by measuring release of ^{32}P -labeled GDP (Ernst et al., 1995).

Step 3 describes GTP-induced dissociation of the $R^* \cdot G$, complex and formation of transducin in its active GTP-bound form. Under conditions in vitro, most of the transducin (mainly the α subunit) leaves the membrane ($G_{\text{tsol}} \cdot \text{GTP}$). Weak binding of GTP to the $R^* \cdot G_{t[\text{empty}]}$ complex induces a conformational change in Gt leading to higher affinity for the nucleotide.

Step 4 describes the hydrolysis of GTP due to the GTPase activity of Gt, which takes minutes at room temperature, but less than 1 sec in rod outer segment (ROS) preparations (Vuong et al., 1991).

3.5.4.2 Binding of Transducin to the SLB

In the dark, transducin was added to the sensor cuvette to a final concentration of $4.5 \mu\text{M}$ (indicated by arrow). An increase in response value by ~ 700 arc sec was observed, which saturated after 300 sec (Fig. 30). The binding of Gt to SLB can be reversed by changing the solution buffer in the cuvette.

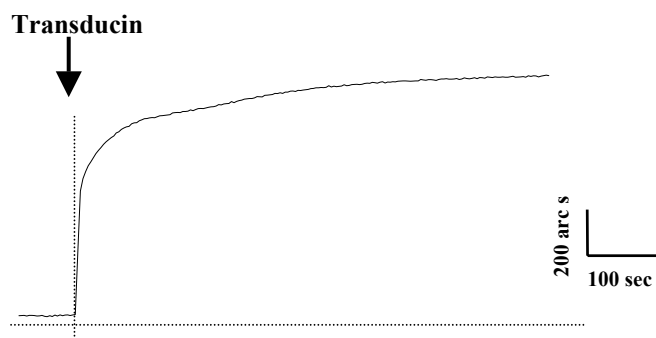


Fig. 30 Sensorgram of Transducin Binding to A Supported Lipid Bilayer Containing Rhodopsin After formation of the SLB by micellar dilution, the buffer in the cuvette was exchanged with buffer G (146 μ l), in which all subsequent steps were carried out. 44 μ l transducin (stock concentration 19.5 μ M) was added to the cuvette to a final concentration of 4.5 μ M and allowed to bind to the SLB, inducing a response shift of 703 ± 44 arc sec (N=9).

3.5.4.3 Sensorgram of Typical Experiment

When GTP was added to a final concentration of 20 μ M (1mM stock solution), no change in response resonance was observed, indicating that the immobilized rhodopsin was in an inactive conformation.

A light illumination ($\lambda \geq 495$ nm, 20sec) was used to activate rhodopsin. In the absence of GTP, a light illumination induced an increase in the resonance angle indicating the formation of $R^* \cdot G_t$ complex (denoted by R_1 , Fig. 31). Addition of GTP (20 μ M final concentration) after illumination triggered a fast decrease in the resonance angle (denoted by R_2), which due to transducin activation and subsequent desorption of $G_t \alpha \cdot GTP$ (and some $G_t \beta \gamma$) from the SLB. R_2 was always less than 60% of R_3 , which indicates the angle shift induced by binding of G_t to the membrane, i. e., less than 60% of the transducin mass desorbed from the membrane upon activation of rhodopsin.

After the fast decrease, the resonance angle slowly increased to the starting level, which was reached after ca. 18 minutes. Additional GTP can not induce another decrease in resonance, reflecting the decay of activated rhodopsin to opsin and all-trans-retinal.

Similar traces were obtained for Rho-Bio1 and Rho-Bio2, indicating binding and activation of Gt by R* (Fig. 31). However, no light-induced binding of G-protein and activation (signal increase and decrease, resp.) can be observed for Rho-Bio3 because of its wrong (upside-down) orientation in the SLB.

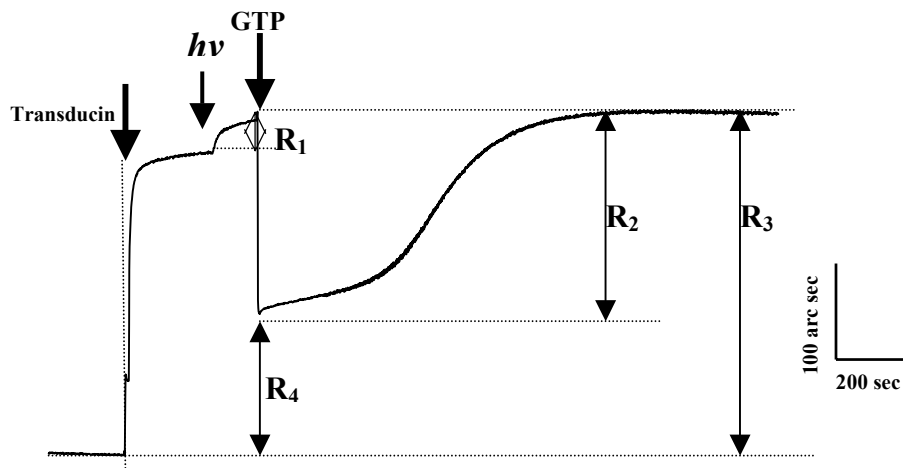


Fig. 31 Sensorgram of Rhodopsin-Gt Interaction After formation of the SLB by micellar dilution, transducin (4.5 μM) was added to the cuvette, inducing a response increase. Light illumination induces formation of $\text{R}^*\cdot\text{G}_{\text{[empty]}}$ complexes, as evidenced by the additional slight resonance angle increase (denoted by R_1); the total change is denoted by R_3 . Addition of GTP (20 μM) leads to a fast desorption of transducin as seen in the fast decrease of the resonance signal immediately after GTP addition. The amplitude of this desorption signal is denoted R_2 . The resonance angle slowly increased and returned almost to the starting value. This is due to GTP hydrolysis and rebinding of Gt to the SLB.

3.5.5 Activation of Rhodopsin

3.5.5.1 Formation of R*·Gt Complex

After transducin binding to the SLB, rhodopsin was activated by illumination (20 sec) with the respective wave-length, usually with $\lambda \geq 495\text{nm}$. This led to a slight increase of the resonance angles described above (3.5.4.3). In the absence of GTP, the activation cascade is stopped at step (3) (see section 3.5.4.1), i.e., the R*·Gt complex is trapped. This positive signal can be compared with the binding signal observed in light scattering experiments when Gt binds from solution to the disc membrane upon light-activation of rhodopsin (Heck et al., 2000 and Schleicher et al., 1987).

In these experiments, activation of rhodopsin in the absence of GTP led to an increase in the mass charge on the membrane: Binding of $G_{t,mb}$ to R* liberates membrane binding places which can be 'refilled' by $G_{t,sol}$. This effect has been readily detected for rhodopsin integrated into supported lipid bilayers, and the measured changes in resonance angle (arc sec) allowed to determine the number of activated rhodopsin molecules per unit area (Heyse et al., 1998).

A similar increase in response value can be detected here: illumination with orange light in the absence of GTP led to a increase in response of $R_1 = 26$ arc sec with Rho-Bio1 (Fig 31), 21 arc sec with Rho-Bio2, no signal can be detected with Rho-Bio3. Because Rho-Bio1 contains both glycosylation sites of wild type rhodopsin, further experiments were done with Rho-Bio1.

3.5.5.2 Rhodopsin Triggered Desorption of Transducin

After illumination, GTP was added to the desired concentration of 20 μM . This induced a fast decrease, followed by a slow relaxation of the response value. The catalytic activity of rhodopsin was denoted by $A_{cat,surf}$, the linear approximation to the time course of the response shift upon rhodopsin catalytic activation, which is given by $A_{cat,surf} = K_{cat}$

•[R*]•[GTP]. A major problem encountered with the investigation of biotin-immobilized rhodopsin was that the observed change of response values showed a relatively high variation between different experiments, although trends were consistent.

To assess $A_{cat,surf}$, the slope of the time course of response value immediately after rhodopsin activation (V_{lin}) was taken. With the same illumination intensity, the derived values for V_{lin} were clearly dependent on the concentration of GTP as expected. At $\lambda \geq 495$ nm and using full flash intensity, V_{lin} of freshly immobilized rhodopsin amounted to 4.05 arc sec/s at a GTP concentration of 2 μ M, and to 12.68 arc s/s for 200 μ M GTP.

Upon the decay of rhodopsin, the $Gt\alpha$ subunit and $Gt\beta\gamma$ combined again with GDP. With another illumination, the newly activated rhodopsin catalyzes again the exchange of GTP for bound GDP, which induces the dissociation of $Gt\alpha$]GTP from $Gt\beta\gamma$]Gt α]GTP. As a result, a fast decrease in resonance angle was observed and thereafter it was followed by a slow increase of response value. This cycle of dissociation and association of Gt can be repeated many times with consecutive illumination steps (Fig. 32).

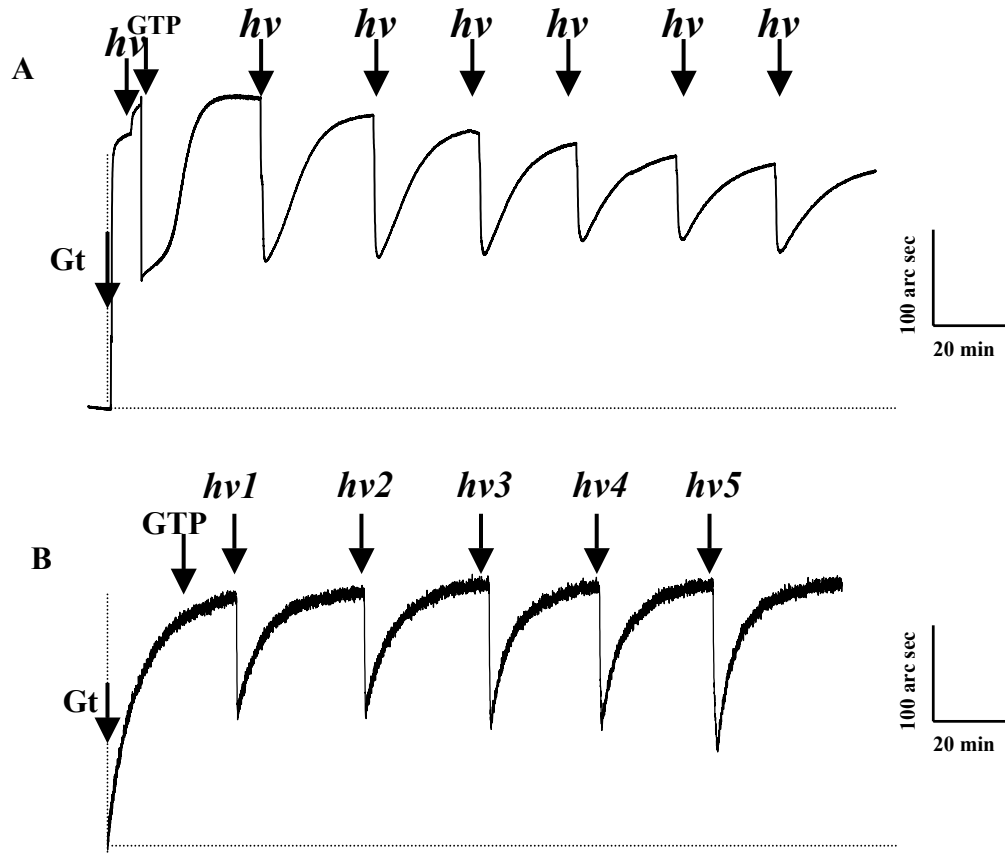


Fig. 32 The Sensorgram of Gt Activation by Rho-Bio1(A) After binding of Gt ($4.5 \mu\text{M}$) for 300 sec to the SBL containing immobilized Rho-Bio1, light illumination was used to activate Rho-Bio1. Addition of GTP ($200 \mu\text{M}$, indicated by an arrow) triggered a fast decrease in the resonance angle, the resonance angle slowly increased to the starting angle after some minutes. Stepwise illumination ($\lambda \geq 495 \text{ nm}$ 20 sec each, indicated by arrow) induce the same repeated activation cycles. (B) In a separate experiment (as in A), no signal decreased can be observed when $100 \mu\text{M}$ GTP was added in the dark to a SLB with bound Gt. Stepwise illumination (indicated by arrows, $\lambda \geq 495 \text{ nm}$ with varying illumination time: $hv1$, 5 sec; $hv2$, 10 sec; $hv3$, 15 sec; $hv4$, 20 sec; $hv5$, 40 sec.) was applied to induce the dissociation signals.

3.5.5.3 Decay of Rhodopsin Activity

Light-activated rhodopsin decays slowly into all-*trans*-retinal and opsin by spontaneous hydrolysis of the connecting Schiff's base. By measuring Trp-fluorescence, it was shown that detergent-solubilized and purified rhodopsin decayed after light activation with a half time of $t_{1/2} = 15.5 \text{ min}$ at pH 6.0 (Farrens et al., 1995). By monitoring the decay of $R^* \cdot Gt$

in native disc membranes by light scattering, a half-time of meta II decay has been determined to be around 20 min at pH 7,5 (Hofmann et al., 1983).

In this experiment, the decay of active rhodopsin is reflected by a slow decrease of the response value R_2 (arc sec) (see fig. 31). We observed that further illuminations after complete return of the resonance angle (reflecting the rebinding of Gt to the SLB), induced again transducin desorption. Addition of GTP without illumination can not induce transducin desorption signal. This shows that the rebinding signal was not due to GTP depletion. Thus, the rebinding signal was due to the Meta II decay and the concomitant decrease of $[R^*]$.

The trace corresponding to rebinding of Gt to SLB, from the minimum to the maximum of the trace of R_2 was fit to a monoexponential function. This yielded $t_{1/2} = 336$ sec. This rate of decay can not directly reflect R^* decay, because GTP would have been depleted after 2-3 rounds which is not observed.

$$y = \frac{R_2}{1 + e^{(x-x_0)/dx}} + R_4$$

X: time (s); Y: R_2 , angle change in resonance (arc sec); dx : differential change of x value; $(x-x_0)$: shift along the x-axis; R_3 : amplitudes of the upper; R_4 : amplitudes of the lower R_2 : difference between upper and lower amplitude (see Fig. 31).

Under the same condition: flash intensity and GTP concentration, each flash activates a fixed proportion of the available rhodopsin. As activated rhodopsin decays to opsin, the amount of activatable rhodopsin is smaller for each consecutive flash. As a consequence, the measured rhodopsin activity decays exponentially with each flash (Fig. 33).

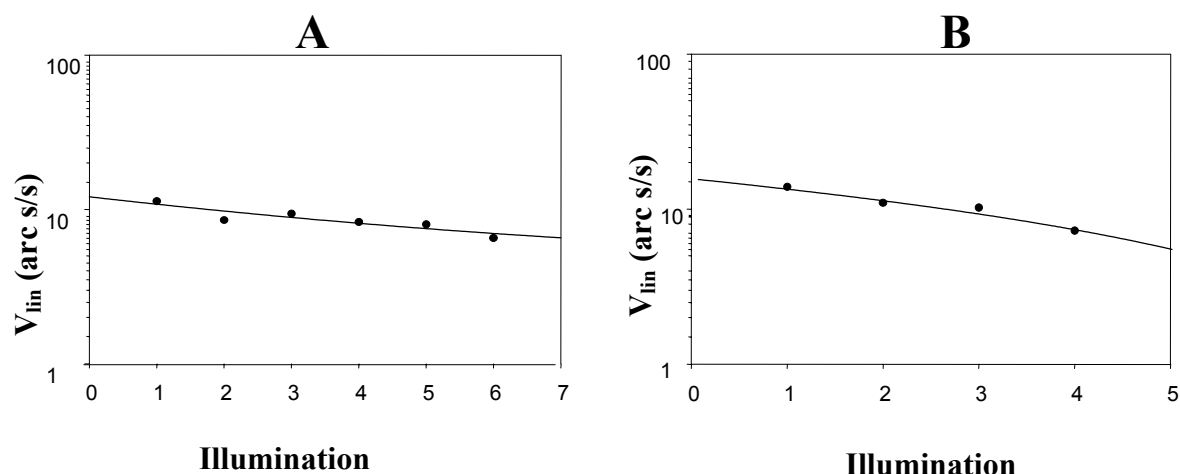


Fig. 33 Decay of rhodopsin Immobilized rhodopsin was activated repeatedly by light illumination ($\lambda \geq 495$ nm, 20sec each, 18 minutes intervals between illuminations; Gt was 1.5 μ M, GTP 100 μ M) (A) The activity of immobilized Rho-Bio decays with each illumination. (B) Also after regeneration of illuminated rhodopsin (from A) with 11-*cis*-retinal, the activity of regenerated rhodopsin decays with each illumination step.

3.5.6 Rhodopsin-Chromophore Interaction

3.5.6.1 The Rhodopsin Cycle

As described before (1.1.2), the opsin/retinal system can be viewed as a prototypic GPCR. The ligand for opsin is 11-*cis*-retinal, which acts as an inverse agonist, suppressing the low basal Gt-activation capacity of opsin (Surya, et al., 1998). Light converts the covalently bound 11-*cis*-retinal by isomerization to a full agonist. Addition of all-*trans*-retinal to opsin also induces a certain rhodopsin activity, however, to a smaller degree, presumably because the functionally important Schiff's base is missing (Jäger, et al., 1996). An antagonist, β -ionone, which corresponds to the ring of the retinal, reduces the binding kinetics of retinal to opsin (Jäger, et al., 1996). Thus, opsin can be investigated with the pharmacological tools of a 'true' GPCR, such as inverse agonists, competitive antagonists, full and partial agonists.

As depicted in Fig. (34), rhodopsin undergoes a cycle with three states: (i) the resting receptor comprising bound 11-*cis*-retinal, (ii) the equilibrium of metarhodopsin states with

inactive meta I and active meta II, both containing all-*trans*-retinal. (iii) the inactivated apo form without chromophore (opsin). The transitions are (a) the photo-isomerization of 11-*cis*-retinal, (b) the cleavage of the Schiff base ($K = 0.003 \text{ sec}^{-1}$) and dissociation of all-*trans*-retinal. (c) the binding of 11-*cis*-retinal and reformation of the Schiff base with the receptor. In vitro, rhodopsin can be stabilized in states (i) and (iii), and at low temperatures in state (ii). The transitions can be controlled by the intensity and the wavelength of the activating light for (a) and by the concentration of 11-*cis*-retinal for (c). Hydroxylamine is capable of accelerating (b) by catalyzing the cleavage of the Schiff base.

This chapter examines whether immobilized and photoactivated rhodopsin is capable to bind 11-*cis*-retinal.

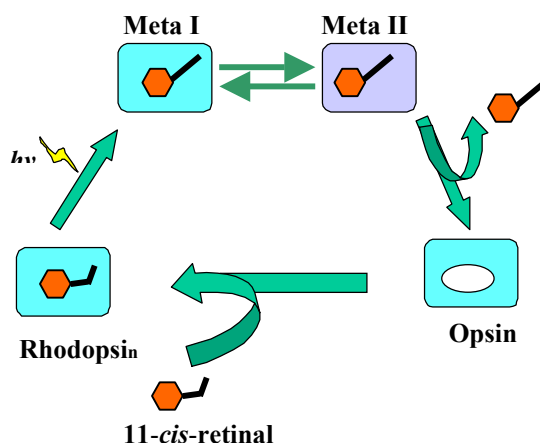


Fig. 34 The Rhodopsin Cycle Three states of a simplified rhodopsin cycle: Rhodopsin, meta-rhodopsin (an equilibrium between meta I and meta II) and opsin, details see text.

3.5.6.2 Regeneration of Rhodopsin from Opsin

In vitro, mixing of stoichiometric amounts (at micromolar concentrations) of 11-*cis*-retinal and opsin has been shown to generate rhodopsin (Basinger, et al., 1973). Retinal can be added to opsin in aqueous solution by adding an ethanolic solution of the chromophore (Jäger et al., 1996). In other protocols, the retinal is incorporated into membranes of vesicles, and the latter are used as vehicles (Melia et al., 1997). It is reasonable to assume that in the case of SLBs, retinal injected into the cuvette will partition into the SLB.

Addition of retinal to SLBs at a final concentration of 5 μM induced an increase of response value, presumably due to its integration into the SLBs (Fig. 35).

First, it was tested if conversion of opsin to rhodopsin could be achieved with the immobilized receptor. Rho-Bio1 was immobilized in the SLB as usual, in the presence of Gt and GTP, and ten consecutive light illuminations ($\lambda \geq 495 \text{ nm}$, 20 sec each, 18 minutes intervals; GTP concentration 200 μM) were applied to activated all available Rho-Bio1. Then, 11-*cis*-retinal was applied to a final concentration of 5 μM and allowed to bind to opsin for 30 minutes (Fig. 35), leading to a small increase in response and then decrease after some minutes, presumably because of the integration of retinal into the membrane and the re-establishment of the membrane binding equilibrium.

After addition of GTP (200 μM final concentration), stepwise illuminations (20 sec each) induced a decrease in the resonance angle similar to the signals obtained before regeneration with retinal. This showed that Rho-Bio1 had been reformed by 11-*cis*-retinal and the immobilized opsin. Further multiple activation cycles as seen after initial illumination of the immobilized rhodopsin: shows that in SLBs, 11-*cis*-retinal is able to largely convert opsin to rhodopsin (Fig.35).

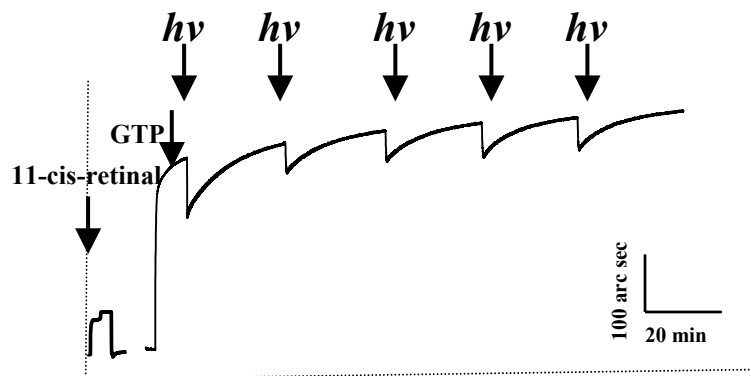


Fig. 35 Regeneration of Rhodopsin In the presence of transducin (1.5 μM) and 200 μM GTP, Rho-Bio1 was completely activated with ten consecutive illumination steps ($\lambda \geq 495 \text{ nm}$, $10 \times 20 \text{ sec}$ in 18 minutes intervals (not shown). Then 5 μM 11-*cis*-retinal was added and allowed to incubate for 30 minutes for regeneration of rhodopsin. Addition of 200 μM GTP (indicated by an arrow) and stepwise illumination (20 sec each) were used to test the activity of the regenerated Rho-Bio1. It showed the same activation cycles compared to the initially immobilized Rho-Bio1.

3.5.6.3 Binding of Chromophore to Opsin

Binding of the chromophore to opsin depends on the concentration of 11-*cis*-retinal (Bieri et al., 1999), the concentration-dependency was assessed by a series of regeneration experiments. After an initial measurement of its activity, the immobilized Rho-Bio1 was activated by ten illumination steps in intervals of 18 minutes. Afterwards, 11-*cis*-retinal was added to the appropriate concentration, allowing 11-*cis*-retinal to bind to opsin for 30 minutes. Thereafter, the buffer in the cuvette was exchanged with fresh G buffer containing the same concentration of Gt and GTP (to prevent depletion of the two by dilution effects), and the regenerated activity was measured by a light-activation of regenerated rhodopsin. All newly formed rhodopsin was again activated completely allowed to decay and regenerated following the same protocol.

The activities of regenerated rhodopsin were estimated by the initial slope immediately after the illumination, and the amount of retrieved activities were compared to that of original rhodopsin (Fig. 36).

3.5.6.4 Stability of Immobilized Opsin

The apoprotein opsin is known to be less stable than rhodopsin. Therefore, it was tested whether the immobilized rhodopsin/opsin could sustain longer experimental times and repeated activation/deactivation cycles.

Immobilized rhodopsin was first subjected to a normal activation (without exogenous 11-*cis*-retinal) to measure the initial activity. The immobilized Rho-Bio1 was activated with five consecutive illuminations ($\lambda \geq 495$ nm, 20 sec) with addition of GTP to a concentration of 200 μ M.

11-*cis*-retinal was injected to a final concentration of 5 μ M. The subsequent increase in the resonance angle is due to the integration of the hydrophobic retinal into the SLB. The system was left to undergo retinal binding for 30 min before a new illumination was applied to test the activity of the freshly reformed rhodopsin. The regenerated activity (estimated by the initial slope after flash) amounted to 80% of the initially measured

activity. To test the stability of the whole system (immobilized rhodopsin, SLB, G protein), three illumination steps ($\lambda \geq 495$ nm, 20 sec) were applied in intervals of ~ 18 min and three activation /deactivation cycles were performed. The activities induced by these light illuminations were strikingly stable (Fig. 37), even though no fresh G protein was added during this time.

This showed that immobilized rhodopsin could cycle through activation/deactivation cycles several times without losing significantly its functionality.

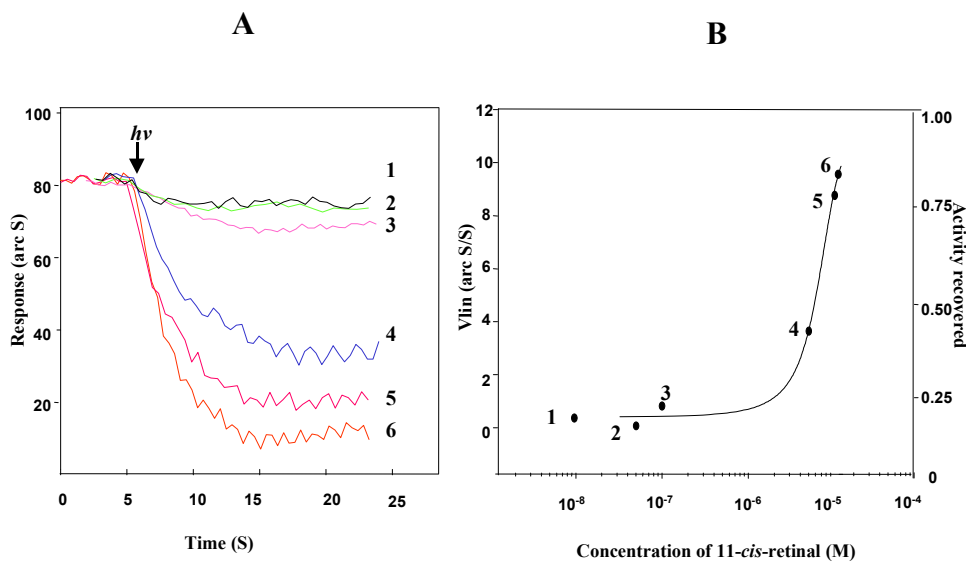


Fig. 36 Binding of 11-cis-retinal to Immobilized Rho-Bio1 The immobilized Rho-Bio was bleached by ten consecutive illuminations (20 sec each) in the presence of 2.5 μ M Gt and 200 μ M GTP. 11-cis-retinal was added to the indicated concentration and allowed to bind for 30 minutes. The activities of regenerated rhodopsin is reflected in the slope of the signal observed after a light illumination ($\lambda \geq 495$ nm, 20 sec). Using the same SLB with rhodopsin, this was repeated for each concentration. (A): recorded resonance traces. (B): Dose-response curve. The slope measured upon the different activations are plotted versus the concentration of added 11-cis-retinal. The scale on the right gives the fraction of the original activity which was regenerated by the respective illumination, showing that at high concentrations of 11-cis-retinal, almost the same rhodopsin activity was obtained comparing to that of freshly immobilized rhodopsin. Numbers indicate different concentration of 11-cis-retinal: 1, 0.01 μ M; 2, 0.05 μ M; 3, 0.1 μ M; 4, 0.5 μ M; 5, 5 μ M; 6, 10 μ M.

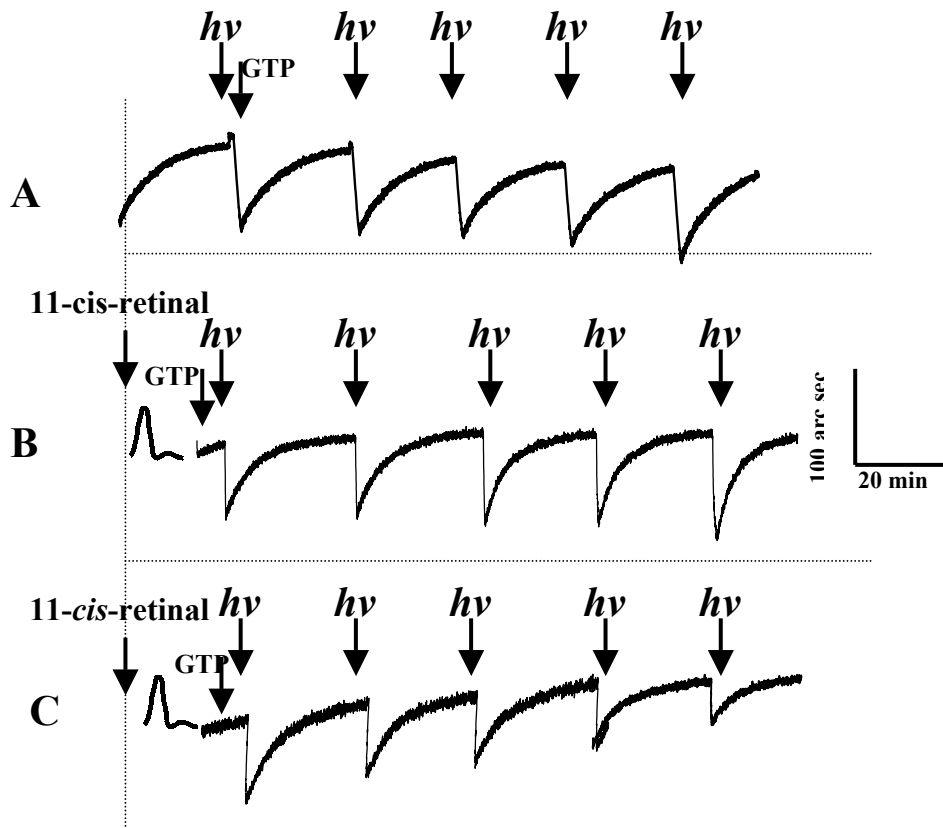


Fig. 37 Sensorgram of Stability of Immobilized Rhodopsin

(A) After binding of Gt (2.5 μM) to the SLB, the immobilized rhodopsin was activated by five consecutive illumination steps ($\lambda \geq 495$ nm, 20 sec each, indicated by arrows). After the first illumination, 200 μM GTP was added (indicated by an arrow), and light illumination steps were applied in intervals of ~ 18 minutes.

(B) Then 11-*cis*-retinal was added (indicated by an arrow) for regeneration of rhodopsin from opsin, and the solution in cuvette was exchanged to buffer R containing 2.5 μM Gt and 200 μM GTP. Regenerated rhodopsin was activated by light illumination steps in intervals of ~ 18 minutes.

(C) 11-*cis*-retinal was added (indicated by an arrow) for the second regeneration of rhodopsin. The reformed rhodopsin showed the similar traces as in A and B. Thus, three activation / deactivation cycles were performed.